J Appl Electrochem (2013) 43:679–687
DOI 10.1007/s10800-013-0547-0

ORIGINAL PAPER

Determination of *p*-nitrophenol on carbon paste electrode modified with a nanoscaled compound oxide Mg(Ni)FeO

Yanhong Xu · Yulong Wang · Yaping Ding · Liqiang Luo · Xiaojuan Liu · Yunxiao Zhang

Received: 4 February 2013 / Accepted: 4 April 2013 / Published online: 30 April 2013

Abstract A novel electrochemical sensor for the determination of *p*-nitrophenol (PNP) was fabricated with the nanoscaled composite oxide Mg(Ni)FeO-modified carbon paste electrode (CPE), and its electrocatalytic performances were investigated using the cyclic voltammogram and differential pulse voltammetry techniques. The influential factors were optimized such as the mass ratio of Mg(Ni)FeO to graphite, the pH value of buffer solution and the accumulation time at open circuit. The indirect oxidation peak current of PNP was found to be proportional to its concentration between 2.0×10^{-6} and 2.0×10^{-4} M on the proposed sensor Mg(Ni)FeO/CPE under the optimal condition (10 % Mg(Ni)FeO/graphite, pH 5.0 HAc–NaAc, 120 s quiescence). The sensor Mg(Ni)FeO/CPE exhibited a high sensitivity of 811 μA mM^{-1} cm^{-2} and a low detection limit of 0.2 μM ($S/N- = 3$) for PNP detection, and got satisfactory results when it was applied to determine PNP in real samples. The results demonstrate that Mg(Ni)FeO/CPE based on the nanomaterial Mg(Ni)FeO with high specific area and mesoporous structure could be employed as an electrochemical sensor for PNP determination with simplicity, low cost, good selectivity, repeatability, and stability.

Y. Xu · Y. Wang · Y. Ding (✉) · L. Luo · X. Liu
College of Sciences, Shanghai University, Shanghai 200444, People's Republic of China
e-mail: wdingyp@sina.com

Y. Xu
School of Life Sciences, Shanghai University, Shanghai 200444, People's Republic of China

Y. Zhang
Shandong Keyuan Chemical Co., Ltd, Laizhou 261413, Shandong, People's Republic of China

Keywords Nanomaterial · Carbon paste electrode · Sensor · *p*-Nitrophenol · Electrochemistry

1 Introduction

The phenolic compounds usually generated by a number of polluting processes including those in the manufacturing chemical industry and agricultural practices have toxic effects on humans, animals, and plants. Comas, convulsions, cyanosis, and even death can result from overexposure to these substances through inhalation, ingestion, eye or skin contact, and absorption through the skin [1]. Phenolic compounds are considered as priority pollutants since these are harmful toward organisms at low concentrations. Especially, the *p*-nitrophenol (PNP), which is as an intermediate or a final product in the most degradation pathways of organophosphorous pesticides [2], has high environmental impact on humans due to its persistence and toxicity [3]. Moreover, PNP is highly soluble in water and is found in both terrestrial and aquatic environments [4]. The existence of this hazardous substance in water can cause some physical, chemical, or biological changes in water quality affecting human health adversely [1, 5]. PNP is considered to be a great threatening chemical substance to the environment [6]. Consequently, PNP has been strictly controlled in the water quality standard by many countries [7–10].

Up to now, many analytical methods including spectrophotometric method [11–13], fluorescent spectrometry [14], chromatography [15–17], capillary electrophoresis [18], and electroanalytical techniques [19] have been proposed for PNP determination. Among the methods, electroanalytical techniques offer a promising technique to determine PNP due to the advantages of high efficiency,

easy control, and simple structure [20, 21]. The performance of the electrochemical process strongly depends on the electrode material [22–27]. Various metal oxides have been investigated as electrodes for electrochemical oxidation or degradation of phenols [28–33]. However, the commercial electrodes in use are few due to their relatively high operating cost or defective stability.

Hydrotalcite-like compounds (HT) and their calcined products (HT500) have been used as sorbents for phenols in water, and the calcined sample exhibits more effective in removing phenols from the solution [34]. In this study, a novel sensor (Mg(Ni)FeO/CPE) has been fabricated based on carbon paste electrode (CPE) modified with the nano-scaled material Mg(Ni)FeO derived from MgNiFe-LDH [35], and used to determine PNP by the oxidation of intermediate hydroxylamine via an electrocatalytic method using the cyclic voltammogram (CV) and differential pulse voltammetry (DPV) techniques in HAc-NaAc buffer solution. The proposed sensor Mg(Ni)FeO/CPE is applied to detect the trace amount of PNP in lake water, human urine and fetal bovine serum (Gibco) samples. To the best of our knowledge, the sensor Mg(Ni)FeO/CPE based on the nanomaterial Mg(Ni)FeO is first employed to determine PNP.

2 Experimental

2.1 Reagents and apparatus

All the reagents including PNP (analytical reagent), HAc and NaAc (analytical reagent), NaOH (analytical reagent), graphite powder (spectral reagent), and paraffin oil were purchased from the Sinopharm Group Chemical Reagent Co., Ltd. (Shanghai, China) and all the solutions were made in double distilled water. The material Mg(Ni)FeO was derived from its precursor prepared by coprecipitation method [35], and characterized by X-ray diffraction (XRD) (Rigaku DLMAX-2200 X-ray diffractometer, Cu Kα radiation, $\lambda = 1.5418$ Å, 40 kV, 40 mA, scanning rate: 0.08° s^{-1}) in the range of 10°–70° and low temperature N_2 adsorption and desorption isotherms (American Micromeritics Tristar 3000 system) after outgassing at 200 °C for 2 h. The electrochemical impedance spectroscopy (EIS) measurements (Solartron 1255B Frequency Response analyzer/SI 1287) of the electrodes were performed in a solution of 0.1 M KCl containing 5 mM $Fe(CN)_6^{3-}$/$Fe(CN)_6^{4-}$ (1:1) in the range of 0.1–10^5 Hz.

All electrochemical measurements were carried out on a CHI 660C electrochemical workstation (Shanghai Chenhua Co. Ltd., China). A conventional three-electrode system was employed: a saturated calomel electrode (SCE) as reference, a Pt wire as auxiliary and Mg(Ni)FeO/CPE as working electrode.

2.2 Mg(Ni)FeO/CPE fabrication and PNP measurement

Mg(Ni)FeO/CPE was fabricated by fully mixing appropriate weight of Mg(Ni)FeO with 1.0 g of carbon paste containing 70 % (w/w) graphite powder and 30 % (w/w) paraffin oil. Then, the homogenized mixture was used to pack clean glass tubes of 3 mm inner diameter. The electrical contact was established with the copper stick, and the surface of sensor Mg(Ni)FeO/CPE was polished by gently rubbing over a piece of weighing paper to get a mirror-like surface just before use.

A PNP stock solution (1.0 mM) was prepared and diluted to working solutions with HAc–NaAc buffer solution. Unless otherwise stated, pH 5.0 HAc–NaAc (0.1 M) was used as supporting electrolyte for the determination of PNP. CVs were initially recorded in HAc–NaAc buffer solution and then in the same solution containing 0.8 mM PNP (scan rate: 100 mV s^{-1}). DPVs of PNP (0.08 mM) were recorded from −1.0 to 0.6 V and all electrochemical experiments were carried out at room temperature.

3 Results and discussion

3.1 Characterizations of Mg(Ni)FeO sample and electrodes

XRD of the sample Mg(Ni)FeO is shown in Fig. 1. The synthesized material possesses information of the composite oxide as shown by the two broad diffraction peaks at 2θ (T) of 43° and 62°. Compared with the standard spectrum, the main phases (111) (200) (220) of the sample is composed of MgO (JCPDS 43-1022), $MgNiO_2$ (JCPDS 24-0712), and $Mg_{1-x}Fe_xO$ (JCPDS 35-1393) phases (like MgO phases). Herein, the sample is a type of composite oxide composed of Mg, Ni, and Fe metal cations, where different kinds of metal cations can interact and be identically situated on the structural units. The mean particle size of 15 nm based on (200) and (220) planes at ca. 43° and 62° may be estimated using Scherer's formula $D = 0.89\lambda/(\beta\cos T)$, where D is the crystallite size, λ is the wavelength of the radiation used, T is the Bragg diffraction angle (θ) and β is the value of the full width at half maximum (FWHM), respectively [36].

Figure 2 shows that the adsorption and desorption isotherms of Mg(Ni)FeO and pore size distribution curve in the liquid N_2 temperature. The nanoparticles exhibit N_2 adsorption and desorption isotherms of type IV according to the IUPAC classification [37] (Fig. 2a). The desorption isotherm differs from the adsorption isotherm in the relative pressure (P/P_0) range from 0.75 to 0.97, which is characteristic of mesoporous materials. Specific surface

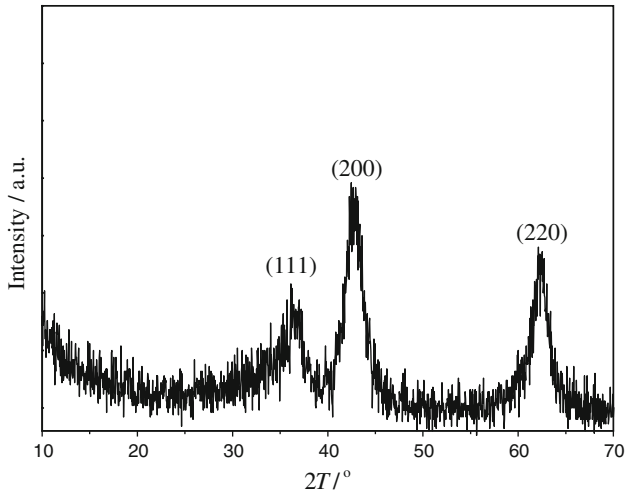

Fig. 1 XRD pattern of the synthesized sample Mg(Ni)FeO

area can be calculated by the Brunauer–Emmett–Teller (BET) method using adsorption isotherms, and the BET surface area of the particles is 88 m^2 g^{-1}. According to the desorption isotherm branch between 1.7 and 300.0 nm diameter, the Barret–Joyner–Halenda (BJH) desorption average pore diameter is 17.9 nm, and the total pore volume is determined to be 0.54 cm^3 g^{-1} by the BJH method (Fig. 2b). Mg(Ni)FeO nanoparticles possess enjoyable properties of high specific surface area and mesoporous structure, which makes it available to achieve high absorption when PNP is determined.

The interface properties of CPE and Mg(Ni)FeO/CPE are characterized by EIS (Fig. 3). EIS is well known as an effective tool for studying electrochemical transformation processes of electrodes [38, 39]. The semicircle diameter in EIS, equal to Nyquist plots (R_{et}), controls the electron transfer kinetics on the electrode interface. As is seen in Fig. 3 the R_{et} of Mg(Ni)FeO/CPE (b) is larger than that of bare CPE (a), suggesting that Mg(Ni)FeO has modified with CPE which may hinder the electroconductivity of CPE.

3.2 Electrochemical studies of PNP

The electrochemical behavior of PNP on the fabricated sensor Mg(Ni)FeO/CPE is studied using CVs after 2 s quiescence. Figure 4I shows the CVs of PNP (0.8 mM) on the bare CPE (curve a′) and Mg(Ni)FeO/CPE (curve b′) in HAc–NaAc (0.1 M, pH 5.0) at the scan rate of 100 mV s^{-1} from −1.2 to +0.6 V. As it can be seen in Fig. 4I, a pair of well-defined redox peaks (O_1/R_2) are observed apparently at ca. +0.22 V on the bare CPE (curve a′) and Mg(Ni)FeO/CPE (curve b′), besides the main reduction peak at −0.85 V, associated with the $\mathbf{4e^-}$ reduction of the nitro group of PNP adsorbed in the electrode surface [3, 40]. As a contrast, there

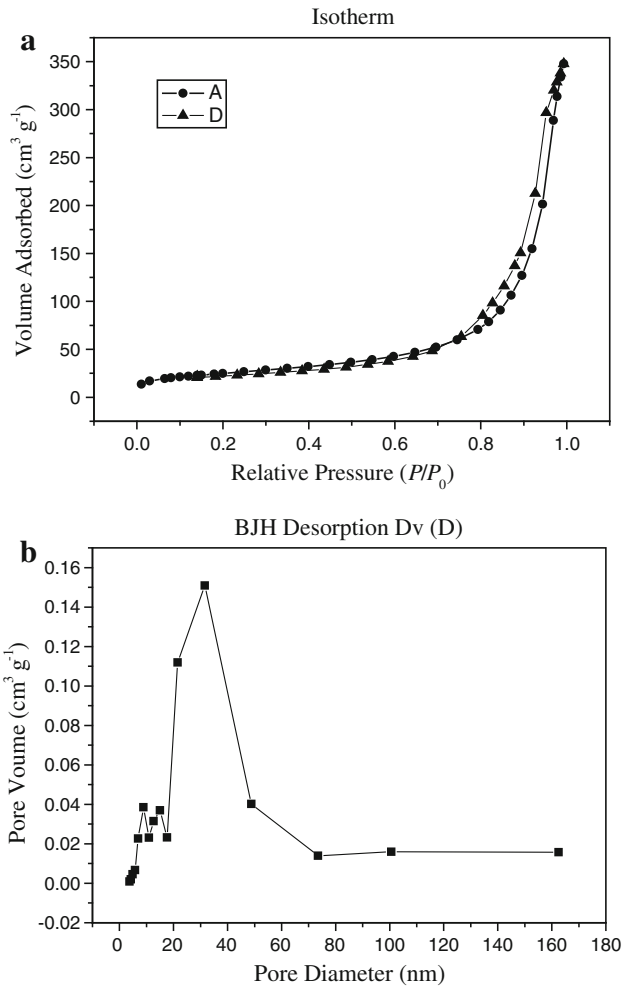

Fig. 2 The low temperature N_2 adsorption and desorption isotherms of Mg(Ni)FeO (**a**) and pore size distribution curve (**b**)

are no redox peaks on the bare CPE or Mg(Ni)FeO/CPE (curve a and b) without PNP in HAc–NaAc. However, the two well-defined peaks and the reduction peak current of PNP on Mg(Ni)FeO/CPE (curve b′) increase obviously compared with those on CPE (curve a′). It may be due to the high specific surface area of Mg(Ni)FeO resulting in high adsorption of PNP that enhances the effect on electrochemical oxidation of PNP.

To obtain further information concerning the reactions occurring at Mg(Ni)FeO/CPE, Fig. 4II, III shows that effect of the different switching potential and the different scan on the reaction behavior of PNP, respectively. In Fig. 4II, five CVs of PNP are obtained on Mg(Ni)FeO/CPE in HAc-NaAc (0.1 M, pH 5.0) at the scan rate of 100 mV s^{-1} for the first scan at different switching potentials from −0.6 to −1.4 V. In the curves, it is apparent that there appears oxide peak between +0.2 and +0.3 V besides the main reduction peak at −0.85 V when the negative potential incursion exceeds −0.8 V, and the

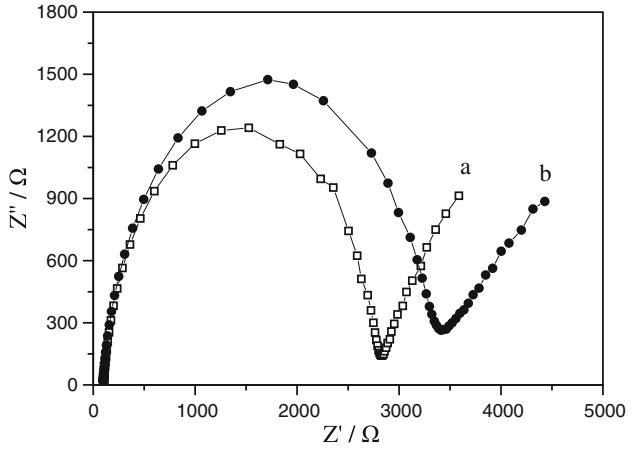

Fig. 3 Nyquist plots for EIS on CPE (**a**) and Mg(Ni)FeO/CPE (**b**) in a solution of 0.1 M KCl with 5 mM $Fe(CN)_6^{3-}/Fe(CN)_6^{4-}$ in the frequency range of 0.1–10^5 Hz

peak current (I_p) of O_1 increases greatly with the potential from −0.8 to −1.0 V and then increases slightly, indicating that I_p of O_1 depends on the potential. Figure 4III depicts the CVs of PNP on Mg(Ni)FeO/CPE at different scans from −1.0 to +0.6 V. The results shows that I_p for the reduction signal R_1 decreases greatly in the successive scans due to the adsorption of hydroxylamine species on the electrode surface. While the oxidation peak O_1 appears in the first scan, and increases in the second scan, remaining almost constant in the following ones. But it is worthwhile noticing that the reduction peak R_2 appears from the second scan, and R_2 increases in the second scan, almost remaining constant in the following ones. The two voltammetric peaks R_2/O_1 are associated with the peak R_1, and the changes of peak currents are consistent with the results reported [3, 41].

Scheme 1 gives the electrochemical catalytic mechanism of PNP, it accounts for the main peaks observed for the CV behaviors of PNP in Fig. 4. In this scheme, R_1 is the result of four-electron reduction of PNP (I) to *p*-hydroxylaminophenol (II), which easily undergoes a two-electron oxidation (O_1) to give the *p*-nitrosophenol (III). On the return scan, the *p*-nitrosophenol (III) is then reduced through a reversible two-electron process to back to the *p*-hydroxylaminophenol (II) producing the redox couple O_1/R_2 [42]. Compared with the direct electrochemical oxidation of PNP, the reversible reaction of species (III)/(II) by two-electron oxidation and reduction is more likely to occur [43, 44]. So, the indirect electro-oxidation of PNP (peak O_1) is studied on the fabricated sensor Mg(Ni)FeO/CPE in this work.

In order to get the electrochemical behavior of adsorbed PNP on Mg(Ni)FeO/CPE, the CVs of Mg(Ni)FeO/CPE are measured in 0.1 M HAc–NaAc (pH 5.0) solution containing 0.1 mM PNP at different scan rates (Fig. 5). As is

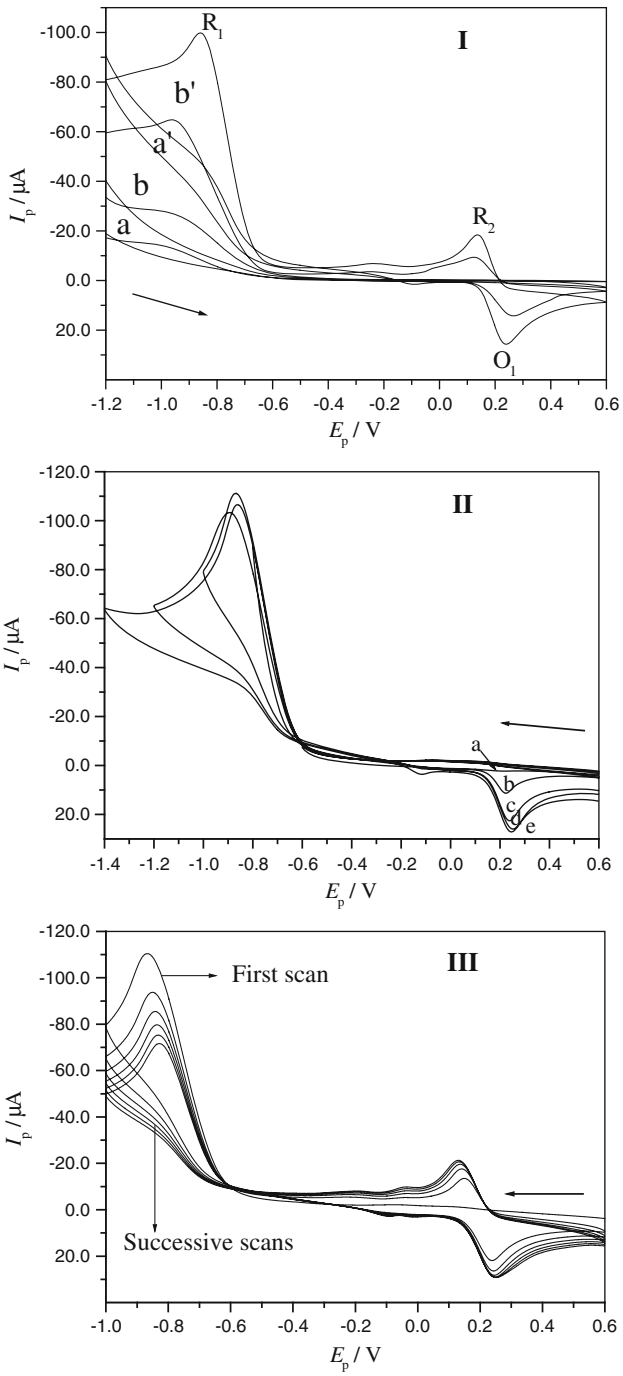

Fig. 4 CVs obtained on the different electrodes in 0.1 M HAc–NaAc solution at pH 5.0 (100 mV s^{-1}): (I) with (a′ and b′) or without (a and b) 0.8 mM PNP from −1.2 to +0.6 V on CPE (a, a′) and Mg(Ni)FeO/CPE (b, b′); (II) effect of different switching potentials on the oxidation currents of PNP on Mg(Ni)FeO/CPE: −0.6 (**a**), −0.8 (**b**), −1.0 (**c**), −1.2 (**d**), −1.4 V (**e**); (III) first scan and five successive scans on Mg(Ni)FeO/CPE from 0.6 to −1.0 V

shown in Fig. 5, all the I_p values of oxidation and reduction peaks increase with the increase of scan rates, and exhibit a linear relation to the square root of the scan rate in the range of 40–500 mV s^{-1} (Fig. 5, inset), indicating that the

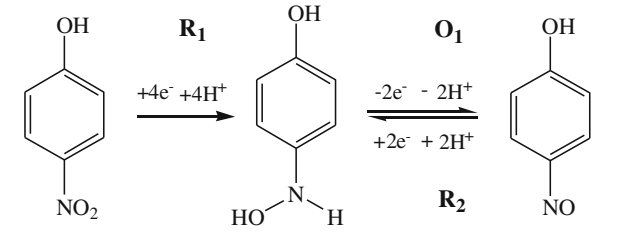

Scheme 1 Electrochemical catalytic mechanism of PNP [3, 42]

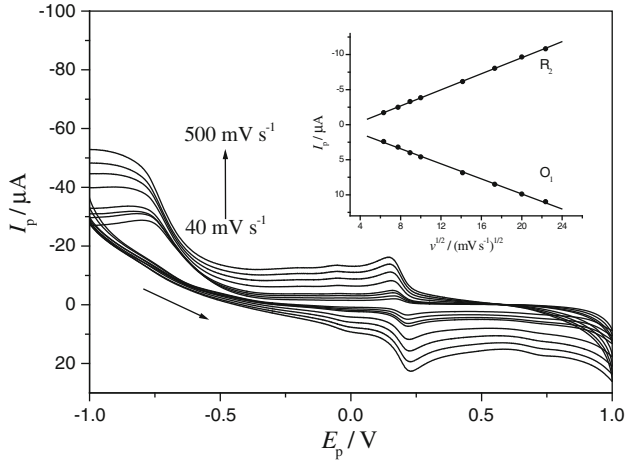

Fig. 5 Influence of scan rates on the peak currents of 0.1 mM PNP at Mg(Ni)FeO/CPE in 0.1 M HAc–NaAc (pH 5.0) solution (inner to outer): 40, 60, 80, 100, 200, 300, 400 and 500 mV s^{-1}; Inset, plot of peak currents versus square roots of different scan rates

reaction of PNP on Mg(Ni)FeO/CPE is a diffusion-controlled process.

3.3 Optimization of operational parameters

The parameters such as the composition of Mg(Ni)FeO/CPE, the pH value of the buffer solution, and the preconcentration time mainly affect the response of PNP on the sensor Mg(Ni)FeO/CPE. So these operational parameters are optimized for PNP (0.08 mM) in 0.1 M HAc–NaAc buffer solution using DPV from −1.0 to 0.6 V (amplitude: 0.05 V, pulse width: 0.05 s, pulse period: 0.2 s).

3.3.1 Influence of pH values

The initial pH value of the supporting electrolyte is an important parameter for the electrochemical behavior of PNP, and influences the adsorption and reaction of PNP on the sensor Mg(Ni)FeO/CPE. To get optimal condition for PNP determination, the effect of pH on the electrochemical behavior of PNP at Mg(Ni)FeO/CPE is studied from 4.0 to

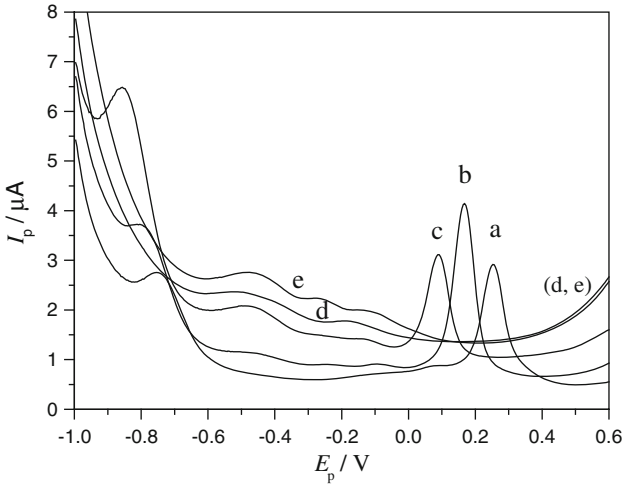

Fig. 6 DPVs of PNP on Mg(Ni)FeO/CPE from −1.0 to 0.6 V in different pH values: pH 4.0 (**a**), pH 5.0 (**b**), pH 6.0 (**c**), pH 7.0 (**d**), pH 8.0 (**e**)

8.0 after 2 s quiescence, and the I_p of O_1 shows very interesting characteristics with respect to pH values as illustrated in Fig. 6. The obvious oxidation peak appears, and the values of I_p and peak potential (E_p) are affected significantly by the pH value. E_p shifts to negative potential (0.25 to 0.08 V) with the pH value increasing, which is consistent with the results reported [17]. I_p increases when pH increases from 4.0 to 5.0, and then decreases from 5.0 to 6.0. Furthermore, when pH increases above 7.0, almost no oxidation peak is observed. At high pH values, it is most probably due to the hydrolysis of the adsorbed intermediate anthraquinones [44] which may cause a dramatic loss in the electrode's surface coverage. The results show that I_p attains maximum at around pH 5.0. So, pH 5.0 is chosen for further studies. On the other hand, three common buffers such as phosphate, Tris–HCl and HAc–NaAc are investigated at pH 5.0. Out of these, HAc–NaAc buffer gives the best response for PNP on Mg(Ni)FeO/CPE, hence is employed as a supporting electrolyte for further studies.

3.3.2 Influence of the composition of Mg(Ni)FeO/CPE

As far as electrode conditions are concerned, the ratio of Mg(Ni)FeO/graphite is an important control factor. Figure 7 shows I_p of PNP at Mg(Ni)FeO/CPE using DPVs (quiet time: 120 s) with different mass ratios of Mg(Ni)-FeO/graphite. The results clearly show that all the values of I_p at modified electrodes is more than that at bare CPE due to the catalytic activity of Mg(Ni)FeO for PNP. I_p of PNP increases with the mass ratio of Mg(Ni)FeO/graphite increase from 0 to 10 %, and then decreases from 10 to 15 %. I_p of PNP attains maximum when the ratio of Mg(Ni)FeO/graphite is 10 %. It is because the increase of the amount of Mg(Ni)FeO nanoparticles with high specific

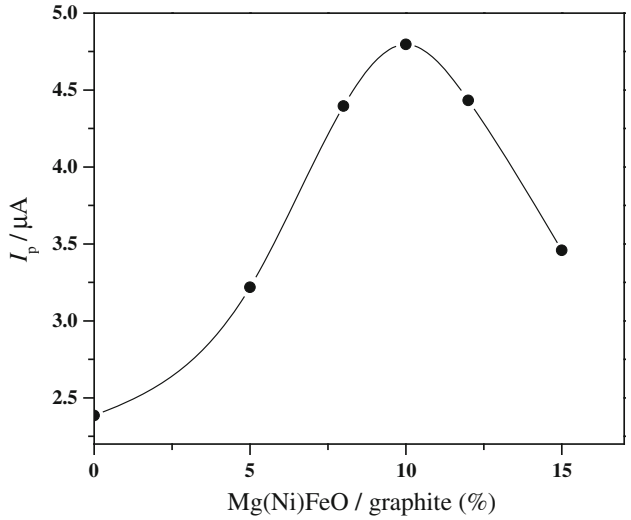

Fig. 7 Influence of the mass content of Mg(Ni)FeO on the I_p of PNP

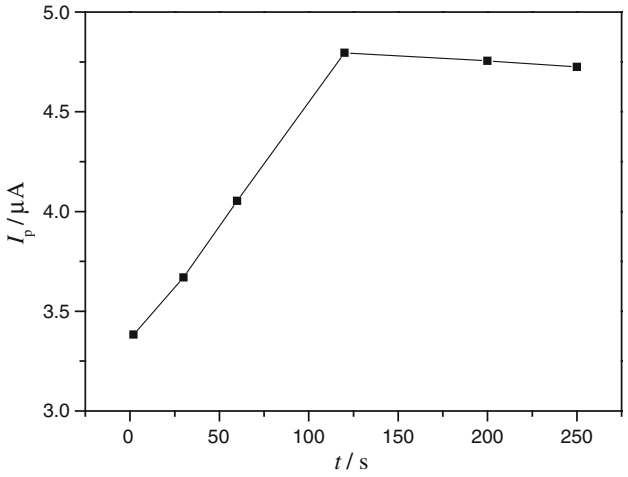

Fig. 8 Influence of the quiet time on the I_p of PNP at the sensor Mg(Ni)FeO/CPE

surface area that increases adsorption and catalytic capacity for PNP, and improves the electro-oxidation of *p*-hydroxylaminophenol on the electrode. However, too many Mg(Ni)FeO may render the electron transfer difficult resulting in a decrease of the current response, which is associated with the larger R_{et} of Mg(Ni)FeO than that of CPE (Fig. 3**).** Therefore, 10 % of Mg(Ni)FeO/graphite is selected for subsequent experiments.

3.3.3 Effect of the quiet time

It is important to choose the quiet time when adsorption studies are undertaken, because it could influence the degree of adsorption of Mg(Ni)FeO/CPE for PNP. The effect of the quiet time at open circuit on the I_p of PNP is investigated using DPV (Fig. 8). I_p increases greatly with the quiet time increasing from 2 to 120 s, which may be due to the high specific area and cavity structure of Mg(Ni)FeO that improves the ability of the electrode to adsorb electroactive PNP. But when the quiet time increases from 120 to 250 s, I_p almost remains constant. The results may be attributed to the equilibrium between species in solution and those adsorbs on the surface of Mg(Ni)FeO/CPE. So, the quiet time of 120 s at open circuit is chosen as the optimal quiet time and used in the following experiments.

3.4 Analytical properties of Mg(Ni)FeO/CPE

Under the optimal condition, the relationship between I_p and the concentration of PNP is examined by DPVs (Fig. 9). It shows that I_p increases greatly with the increase of PNP, and a linear calibration curve for different concentrations of PNP is obtained up to 2.0×10^{-4} M in pH

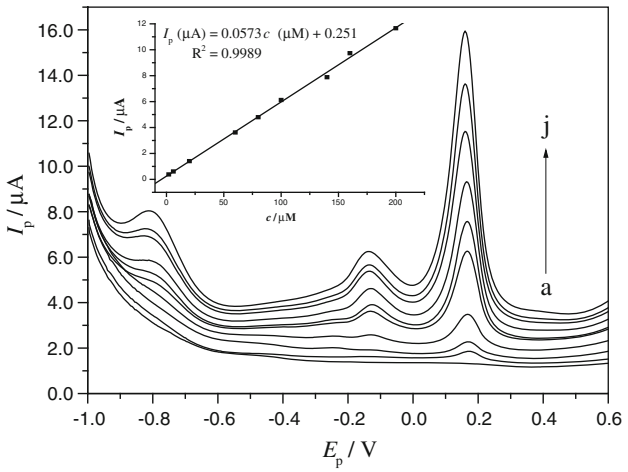

Fig. 9 DPVs of PNP on Mg(Ni)FeO/CPE from −1.0 to 0.6 V in 0.1 M HAc–NaAc (pH 5.0) with different concentrations of PNP (a–j): 0.0, 2.0×10^{-6}, 6.0×10^{-6}, 2.0×10^{-5}, 6.0×10^{-5}, 8.0×10^{-5}, 1.0×10^{-4}, 1.4×10^{-4}, 1.6×10^{-4}, 2.0×10^{-4} M; Insert, calibration curve of PNP on Mg(Ni)FeO/CPE

5.0 HAc–NaAc solution. In the range of 2.0×10^{-6}–2.0×10^{-4} M, the linear equation can be described as follows: I_p (μA) = 0.0573 c (μM) + 0.251 with a correlation coefficient of 0.999 (inset). The sensor exhibits a high sensitivity of 811 μA mM^{-1} cm^{-2} and a low detection limit of 0.2 μM ($S/N = 3$) in the detection of PNP. Comparing with other sensors for the determination of PNP [45–48], this sensor shows superior properties (Table 1).

In order to characterize the stability and reproducibility of Mg(Ni)FeO/CPE, repetitive measurement-regeneration cycles are carried out in 0.08 mM PNP. After each measurement, the electrode is washed thoroughly and dipped into buffer solution and potential sweep are carried out in the same potential window several times until the original

Table 1 Comparison among various electroanalytical methods for the determination of PNP

Samples	Low detection limited (μM)	Sensitivity	Range (μM)	References
(DTD)/Ag/CPE	0.25	~	1–100	[45]
Nafion/GCE	17.1	0.0089 μA μM^{-1}	20–230	[46]
Nanoporous Au electrode	~	0.01046 μC mM cm^{-2}	1.79–72	[47]
Nano-Au/GCE	8	~	7.5–1000	[48]
Mg(Ni)FeO/CPE	0.2	0.0573 μA μM^{-1}	2–200	This work

Table 2 Recovery tests for PNP on Mg(Ni)FeO/CPE in lake water, human urine and blood serum samples

Samples	Spiked PNP in samples/(10^{-5}M)	Found/(10^{-5}M)	Mean R/ % ($n = 3$)	Mean average R ± RSD/ %($n = 3$)
Lake water	–	ND	–	100.2 ± 0.52 %
	6.50	6.48	99.7	
	8.50	8.56	100.7	
	10.50	10.53	100.3	
Human urine	–	ND	–	96.8 ± 2.76 %
	6.50	6.26	96.3	
	8.50	8.28	97.4	
	10.50	10.15	96.7	
Blood serum	–	ND	–	97.4 ± 1.89 %
	6.50	6.31	97.1	
	8.50	8.20	96.5	
	10.50	10.35	98.6	

* *ND* not detected, *R* recovery % ($n = 3$); average recovery % ± RSD % ($n = 3$)

background current is regained. The results of 11 successive measurements show that I_p of PNP gives a relative standard deviation (RSD) of 2.25 %. Thus, the renewal electrode gives a good reproducibility. Moreover, after Mg(Ni)FeO/CPE has been reserved with preservative film at the room temperature for 25 days, Mg(Ni)FeO/CPE is employed to determine PNP, I_p of PNP yields a value of 92 % as that of 25 days before. The sensor Mg(Ni)FeO/CPE for PNP detection has good long-term storage stability and excellent reproducibility.

Various ions are examined with respect to their interference with the determination of PNP. Parathion (200-fold), resorcinol (75-fold), ethanol (50-fold), Ca^{2+} (100-fold), NH_4^+ (100-fold), Zn^{2+} (80-fold), Co^{2+} (30-fold), K^+ (100-fold), SO_4^{2-} (80-fold), and Cl^- (200-fold) do not interference the PNP response within deviations below 5 %. The sensor Mg(Ni)FeO/CPE shows a good selectivity for PNP determination.

3.5 Application of Mg(Ni)FeO/CPE

In order to study the performance of proposed method in practical analytical situations, the fabricated sensor Mg(Ni)FeO/CPE is applied to determine PNP in lake water, human urine, and fetal bovine serum samples, respectively. The three samples analyzed contain no PNP, so they have to be spiked with the analyte at a certain concentration for three times. The recoveries of PNP by standard addition method are listed in Table 2. The results show that the average recovery of PNP is from 96.8 ± 2.76 to 100.2 ± 0.52 %, validating the potential utility of the proposed sensor for PNP detection in the field of environmental monitoring and controlling.

4 Conclusion

A sensor Mg(Ni)FeO/CPE based on the nanoscaled material Mg(Ni)FeO with simplicity and low cost for the electrocatalytic oxidation of PNP has been investigated. The fabricated sensor Mg(Ni)FeO/CPE exhibits good electrochemical properties such as high sensitivity, high stability, high precision, ease of preparation and regeneration, a wide range and a low detection limit. The applicability of the sensor to measure PNP in lake water, human urine and blood serum samples has also been demonstrated, and the results are satisfactory. The proposed sensor Mg(Ni)FeO/CPE offers great promise for rapid detection of PNP for the environmental control, chemical industry and pharmaceutical applications.

Acknowledgments This research is supported by the National Natural Science Foundation of China (Nos. 21271127, 61171033) and the Nano-Foundation of Science and Techniques Commission of Shanghai Municipality (No. 12nm0504200), Leading Academic Discipline Project of Shanghai Municipal Education Commission (J50102), Postdoctoral Foundation of Shanghai University, China.

References

1. Arasteh R, Masoumi M, Rashidi A, Moradi L, Samimi V, Mostafavi S (2010) Adsorption of 2-nitrophenol by multi-wall carbon nanotubes from aqueous solutions. Appl Surf Sci 256(14): 4447–4455
2. Patnaik P, Khoury JN (2004) Reaction of phenol with nitrite ion: pathways of formation of nitrophenols in environmental waters. Water Res 38(1):206–210
3. Moraes FC, Tanimoto ST, Salazar-Banda GR, Machado SAS, Mascaro LH (2009) A new indirect electroanalytical method to monitor the contamination of natural waters with 4-nitrophenol using multiwall carbon nanotubes. Electroanalysis 21(9):1091–1098
4. Zaidi BR, Imam SH (1996) Inoculation of microorganisms to enhance biodegradation of phenolic compounds in industrial wastewater: isolation and identification of three-indigenous bacterial strains. J Gen Appl Microbiol 42(3):249–256
5. Oubiña A, Ballesteros B, Galve R, Barcelo D, Marco MP (1999) Development and optimization of an indirect enzyme-linked immunosorbent assay for 4-nitrophenol. Application to the analysis of certified water samples. Anal Chim Acta 387(3): 255–266
6. Pan L, Xu M, Zhang ZD (2010) A general synthesis and electrocatalytic activity of low-dimensional MO and M–Co (M = Cu, Ni, Zn and Cd) composite oxides. Mater Chem Phys 123(1):293–299
7. Keith L, Telliard W (1979) ES&T special report: priority pollutants: I-a perspective view. Environ Sci Technol 13(4):416–423
8. Barbour MT, Gerritsen J, Snyder B, Stribling J (1999) Rapid bioassessment protocols for use in streams and wadeable rivers. USEPA, Washington
9. Pan B, Chen X, Zhang W, Zhang X, Zhang Q (2006) Preparation of an aminated macroreticular resin adsorbent and its adsorption of *p*-nitrophenol from water. J Hazard Mater 137(2):1236–1240
10. Lee SM, Tiwari D (2012) Organo and inorgano–organo-modified clays in the remediation of aqueous solutions: an overview. Appl Clay Sci 59(60):84–102
11. Fiamegos Y, Stalikas C, Pilidis G, Karayannis M (2000) Synthesis and analytical applications of 4-aminopyrazolone derivatives as chromogenic agents for the spectrophotometric determination of phenols. Anal Chim Acta 403(1–2):315–323
12. Shkumbatiuk R, Bazel YR, Andruch V, Trk M (2005) Investigation of 2-[(E)-2-(4-diethylaminophenyl)-1-ethenyl]-1, 3, 3-trimethyl-3H-indolium as a new highly sensitive reagent for the spectrophotometric determination of nitrophenols. Anal Bioanal Chem 382(6):1431–1437
13. Niazi A, Yazdanipour A (2007) Spectrophotometric simultaneous determination of nitrophenol isomers by orthogonal signal correction and partial least squares. J Hazard Mater 146(1–2): 421–427
14. Wang X, Zeng H, Zhao L, Lin JM (2006) A selective optical chemical sensor for 2,6-dinitrophenol based on fluorescence quenching of a novel functional polymer. Talanta 70(1):160–168
15. Wang SP, Chen HJ (2002) Separation and determination of nitrobenzenes by micellar electrokinetic chromatography and high-performance liquid chromatography. J Chromatogr A 979(1–2): 439–446
16. Borras C, Berzoy C, Mostany J, Herrera J, Scharifker B (2007) A comparison of the electrooxidation kinetics of *p*-methoxyphenol and *p*-nitrophenol on Sb-doped SnO_2 surfaces: concentration and temperature effects. Appl Catal B 72(1–2):98–104
17. Honeychurch KC, Hart JP (2007) Voltammetric behavior of *p*-nitrophenol and its trace determination in human urine by liquid chromatography with a dual reductive mode electrochemical detection system. Electroanalysis 19(21):2176–2184
18. Guo X, Wang Z, Zhou S (2004) The separation and determination of nitrophenol isomers by high-performance capillary zone electrophoresis. Talanta 64(1):135–139
19. Mulchandani P, Hangarter CM, Lei Y, Chen W, Mulchandani A (2005) Amperometric microbial biosensor for *p*-nitrophenol using Moraxella sp.-modified carbon paste electrode. Biosens Bioelectron 21(3):523–527
20. Jüttner K, Galla U, Schmieder H (2000) Electrochemical approaches to environmental problems in the process industry. Electrochim Acta 45(15–16):2575–2594
21. Zhou MH, Dai QZ, Lei LC, Ma C, Wang DH (2005) Long life modified lead dioxide anode for organic wastewater treatment: electrochemical characteristics and degradation mechanism. Environ Sci Technol 39(1):363–370
22. Kötz R, Stucki S, Carcer B (1991) Electrochemical waste water treatment using high overvoltage anodes. Part I: physical and electrochemical properties of SnO_2 anodes. J Appl Electrochem 21(1):14–20
23. Sanghavi BJ, Srivastava AK (2013) Adsorptive stripping voltammetric determination of imipramine, trimipramine and desipramine employing titanium dioxide nanoparticles and an amberlite XAD-2 modified glassy carbon paste electrode. Analyst 138(5):1395–1404
24. Sanghavi BJ, Mobin SM, Mathur P, Lahiri GK, Srivastava AK (2013) Biomimetic sensor for certain catecholamines employing copper(II) complex and silver nanoparticle modified glassy carbon paste electrode. Biosens Bioelectron 39(1):124–132
25. Sanghavi BJ, Srivastava AK (2010) Simultaneous voltammetric determination of acetaminophen, aspirin and caffeine using an in situ surfactant-modified multiwalled carbon nanotube paste electrode. Electrochim Acta 55(28):8638–8648
26. Babaei A, Khalilzadeh B, Afrasiabi M (2010) A new sensor for the simultaneous determination of paracetamol and mefenamic acid in a pharmaceutical preparation and biological samples using copper(II) doped zeolite modified carbon paste electrode. J Appl Electrochem 40(8):1537–1543
27. Yang S, Qu L, Yang R, Li J, Yu L (2010) Modified glassy carbon electrode with nafion/MWNTs as a sensitive voltammetric sensor for the determination of paeonol in pharmaceutical and biological samples. J Appl Electrochem 40(7):1371–1378
28. Feng YJ, Li XY (2003) Electro-catalytic oxidation of phenol on several metal-oxide electrodes in aqueous solution. Water Res 37(10):2399–2407
29. Quiroz MA, Reyna S, Martinez-Huitle CA, Ferro S, De Battisti A (2005) Electrocatalytic oxidation of *p*-nitrophenol from aqueous solutions at Pb/PbO_2 anodes. Appl Catal B 59(3–4):259–266
30. Li XY, Cui YH, Feng YJ, Xie ZM, Gu JD (2005) Reaction pathways and mechanisms of the electrochemical degradation of phenol on different electrodes. Water Res 39(10):1972–1981
31. Li M, Feng CP, Hu WW, Zhang ZY, Sugiura N (2009) Electrochemical degradation of phenol using electrodes of Ti/RuO_2–Pt and Ti/IrO_2–Pt. J Hazard Mater 162(1):455–462
32. Adams B, Tian M, Chen A (2009) Design and electrochemical study of SnO_2-based mixed oxide electrodes. Electrochim Acta 54(5):1491–1498
33. Wang YQ, Gu B, Xu WL (2009) Electro-catalytic degradation of phenol on several metal-oxide anodes. J Hazard Mater 162(2–3):1159–1164

34. Ulibarri MA, Pavlovic I, Hermosín MC, Cornejo J (1995) Hydrotalcite-like compounds as potential sorbents of phenols from water. Appl Clay Sci 10(1–2):131–145
35. Xu YH, Liu XJ, Ding YP, Luo LQ, Wang YL, Zhang Y, Xu YH (2011) Preparation and electrochemical investigation of a nanostructured material Ni^{2+}/MgFe layered double hydroxide as a glucose biosensor. Appl Clay Sci 52(3):322–327
36. Patterson AL (1939) The Scherrer formula for X-ray particle size determination. Phys Rev 56(10):978–982
37. Sing K, Everett D, Haul R, Moscou L, Pierotti R, Rouquerol J, Siemieniewska T (1985) Reporting physisorption data for gas/solid systems, with special reference to the determination of surface area and porosity (recommendations 1984). Pure Appl Chem 57(4):603–619
38. Baranski AS, Krogulec T, Nelson LJ, Norouzi P (1998) High-frequency impedance spectroscopy of platinum ultramicroelectrodes in flowing solutions. Anal Chem 70(14):2895–2901
39. Li FH, Wang W (2010) Studies on the electrochemical reduction processes of $HTeO_2^+$ by CV and EIS. J Appl Electrochem 40(11):2005–2012
40. Lawrence NS, Pagels M, Meredith A, Jones TGJ, Hall CE, Pickles CSJ, Godfried HP, Banks CE, Compton RG, Jiang L (2006) Electroanalytical applications of boron-doped diamond microelectrode arrays. Talanta 69(4):829–834
41. Zen JM, Jou JJ, Senthil Kumar A (1999) A sensitive voltammetric method for the determination of parathion insecticide. Anal Chim Acta 396(1):39–44
42. Sanghavi BJ, Hirsch G, Karna SP, Srivastava AK (2012) Potentiometric stripping analysis of methyl and ethyl parathion employing carbon nanoparticles and halloysite nanoclay modified carbon paste electrode. Anal Chim Acta 735:37–45
43. Nicholson RS, Shain I (1965) Theory of stationary electrode polarography for a chemical reaction coupled between two charge transfers. Anal Chem 37(2):178–190
44. Hu S, Xu C, Wang G, Cui D (2001) Voltammetric determination of 4-nitrophenol at a sodium montmorillonite–anthraquinone chemically modified glassy carbon electrode. Talanta 54(1):115–123
45. Rounaghi G, kakhki RM, Azizi-toupkanloo H (2012) Voltammetric determination of 4-nitrophenol using a modified carbon paste electrode based on a new synthetic crown ether/silver nanoparticles. Mater Sci Eng C 32(2):172–177
46. Calvo-Marzal P, Rosatto SS, Granjeiro PA, Aoyama H, Kubota LT (2001) Electroanalytical determination of acid phosphatase activity by monitoring *p*-nitrophenol. Anal Chim Acta 441(2):207–214
47. Liu Z, Du J, Qiu C, Huang L, Ma H, Shen D, Ding Y (2009) Electrochemical sensor for detection of *p*-nitrophenol based on nanoporous gold. Electrochem Comm 11(7):1365–1368
48. Chu L, Han L, Zhang XL (2011) Electrochemical simultaneous determination of nitrophenol isomers at nano-gold modified glassy carbon electrode. J Appl Electrochem 41(6):687–694